Supplementary content

Sword-like CuO/CeO_2 composites derived from Ce-BTC metal organic framework with superior CO oxidation performance

Yin Wang [a], Yiqiang Yang [a], Ning Liu [a], Yuxin Wang [b], Xiaodong Zhang [a, *]

[a] School of Environment and Architecture, University of Shanghai for Science and Technology, Shanghai 200093, China

[b] Institute of Applied Biotechnology, Taizhou Vocation & Technical College, Taizhou Zhejiang 318000, China

* To whom correspondence should be addressed. Tel. +86 15921267160, Fax. +86 021 55275979

E-mail address: fatzhxd@126.com, zhangxiaodong@usst.edu.cn (X.D. Zhang)

Table S1 Physicochemical properties of CuCe-BTC materials

Catalysts	BET ($m^2 g^{-1}$)	Pore volume ($cm^3 g^{-1}$)	Pore size (nm)
CuCeBTC-2	101	0.25	1.3~4
CuCeBTC-5	120	0.28	1.3~4
CuCeBTC-10	143	0.31	0.5~4
CuCeBTC-20	194	0.23	0.5~4
Ce-BTC [1]	42	0.085	1.5~2

Table S2 Surface elemental composition and states of CuO/CeO_2 catalysts determined by XPS results

Catalysts	Surface composition (at.%)				O_{latt} (%)	O_{ads} (%)	O_{OH} (%)	$Cu^{+/0}$ (%)	Cu^{2+} (%)
	Cu2p	Ce3d	O1s	C1s					
CuCeO-2	4.51	17.97	54.16	23.36	60.3	18.2	21.5	48	52
CuCeO-5	5.07	16.59	53.61	24.73	72	17.2	10.8	70	30
CuCeO-10	5.55	16.94	52.4	25.11	69	10.8	20.2	63	27
CuCeO-20	8.61	15.19	51.13	25.07	64	10.3	25.7	54	46
CeO_2 [2]	—	12.27	50.19	37.54	91.7	8.3	—	—	—

Table S3 H_2 consumption amount and reduction temperature of CuO/CeO_2 catalysts

Catalysts	α peak		β peak		γ peak	
	H_2 consumption ($\mu molg^{-1}$)	Peak temperature (^oC)	H_2 consumption ($\mu molg^{-1}$)	Peak temperature (^oC)	H_2 consumption ($\mu molg^{-1}$)	Peak temperature (^oC)
CuCeO-2	373	150	907	165	619	193
CuCeO-5	1030	146	1994	175	186	204
CuCeO-10	1122	150	4030	176	211	214
CuCeO-20	2364	182	5791	212	346	251

Table S4 Catalytic activities for CO oxidation of CuO/CeO_2 catalysts derived from MOFs

Catalysts	Synthesis method	Morphology	Cu content (%)	Space volocity (mL h^{-1} g^{-1})	T_{100}(°C)	References
CuO/CeO_2	In-situ solvothermal method	Sword	4.18	18000	100	This work
$CuO\text{-}CeO_2$	Incipient wetness impregnation method	Irregular particle	-	20000	150	20
$CeO_2:Cu^{2+}$	In-situ solvothermal method	Nanorods made up of many particles	10	60000	200	21
$CuO@CeO_2$	Incipient wetness impregnation method	Irregular spherical particle	30	48000	95	33

Supplementary caption

Fig. S1 XRD patterns of CeBTC (a), CuBTC (b), CuCeBTC-2 (c), CuCeBTC-5 (d), CuCeBTC-10 (e) and CuCeBTC-20 (f).

Fig. S2 TG curves of CeBTC (a), CeCuBTC-5 (b), CeCuBTC-10 (c) and CeCuBTC-20 (d).

Fig. S3 N_2 adsorption-desorption isotherms (A) and corresponding pore size distributions (B) of CeBTC (a), CuCeBTC-2 (b), CuCeBTC-5 (c), CuCeBTC-10 (d) and CuCeBTC-20 (e).

Fig. S4 SEM images of CeBTC (a), CeCuBTC-2 (b), CeCuBTC-5 (c), CeCuBTC-10 (d) and CeCuBTC-20 (e).

Fig. S5 N_2 adsorption-desorption isotherms (A) and corresponding pore size distributions (B) of CeO_2 (a), CuCeO-2 (b), CuCeO-5 (c), CuCeO-10 (d) and CuCeO-20 (e).

Fig. S6 XRD results of CuCeO-5 before (a) and after (b) CO oxidation reaction

Fig. S7 TEM result of CuCeO-5 after CO oxidation reaction

Fig. S8 Catalytic activities for CO oxidation of CuCeO-2 (A), CuCeO-5 (B), CuCeO-10 (C) and CuCeO-20 (D) reused for three times

Fig. S9 catalytic activities for CO oxidation at different space velocities (30000 mL h^{-1} g^{-1} (A), 60000 mL h^{-1} g^{-1} (B)) of CuCeO-2 (a), CuCeO-5 (b), CuCeO-10 (c) and CuCeO-20 (d).

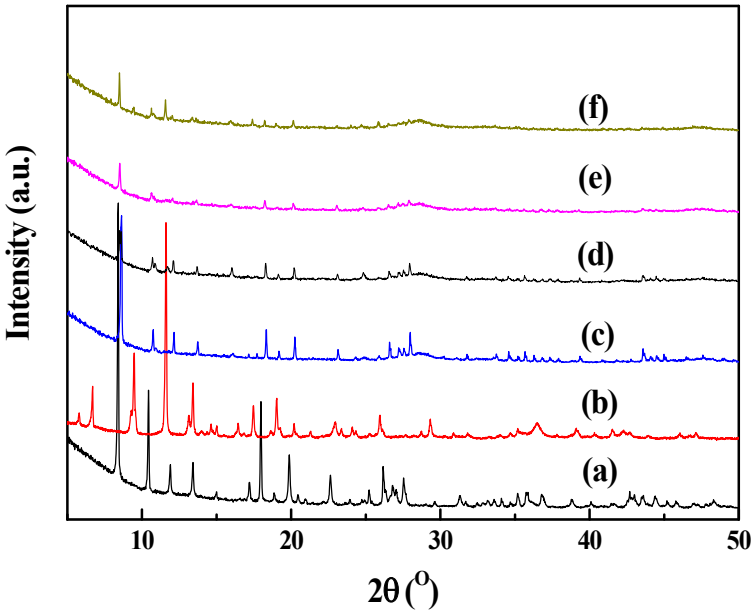

Fig. S1 XRD patterns of CeBTC (a), CuBTC (b), CuCeBTC-2 (c), CuCeBTC-5 (d), CuCeBTC-10 (e) and CuCeBTC-20 (f).

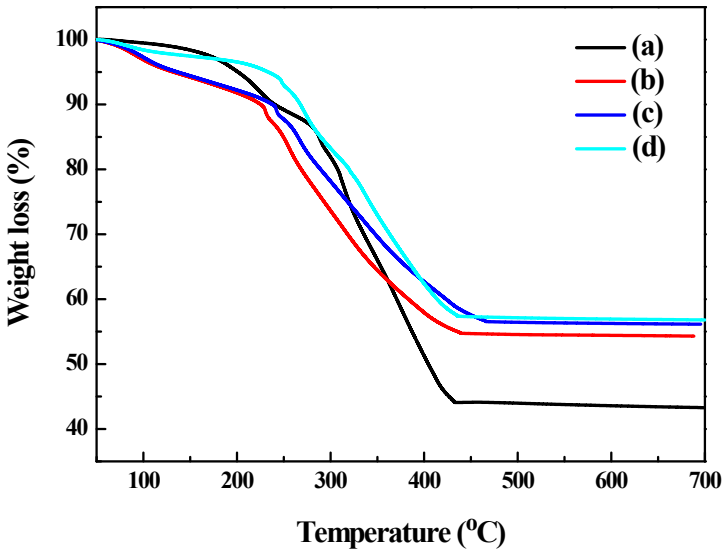

Fig. S2 TG curves of CeBTC (a), CeCuBTC-5 (b), CeCuBTC-10 (c) and CeCuBTC-20 (d).

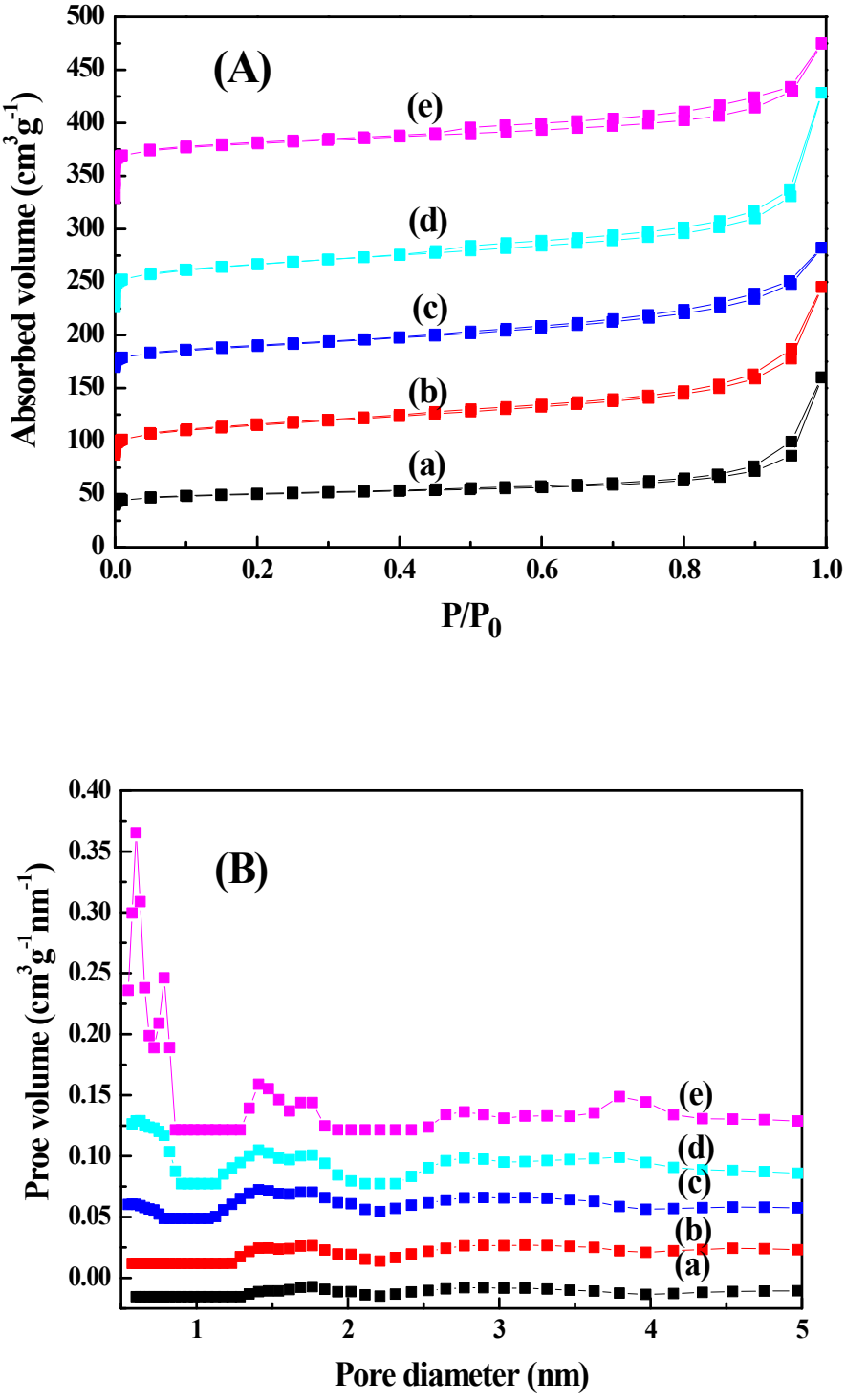

Fig. S3 N_2 adsorption-desorption isotherms (A) and corresponding pore size distributions (B) of CeBTC (a), CuCeBTC-2 (b), CuCeBTC-5 (c), CuCeBTC-10 (d) and CuCeBTC-20 (e).

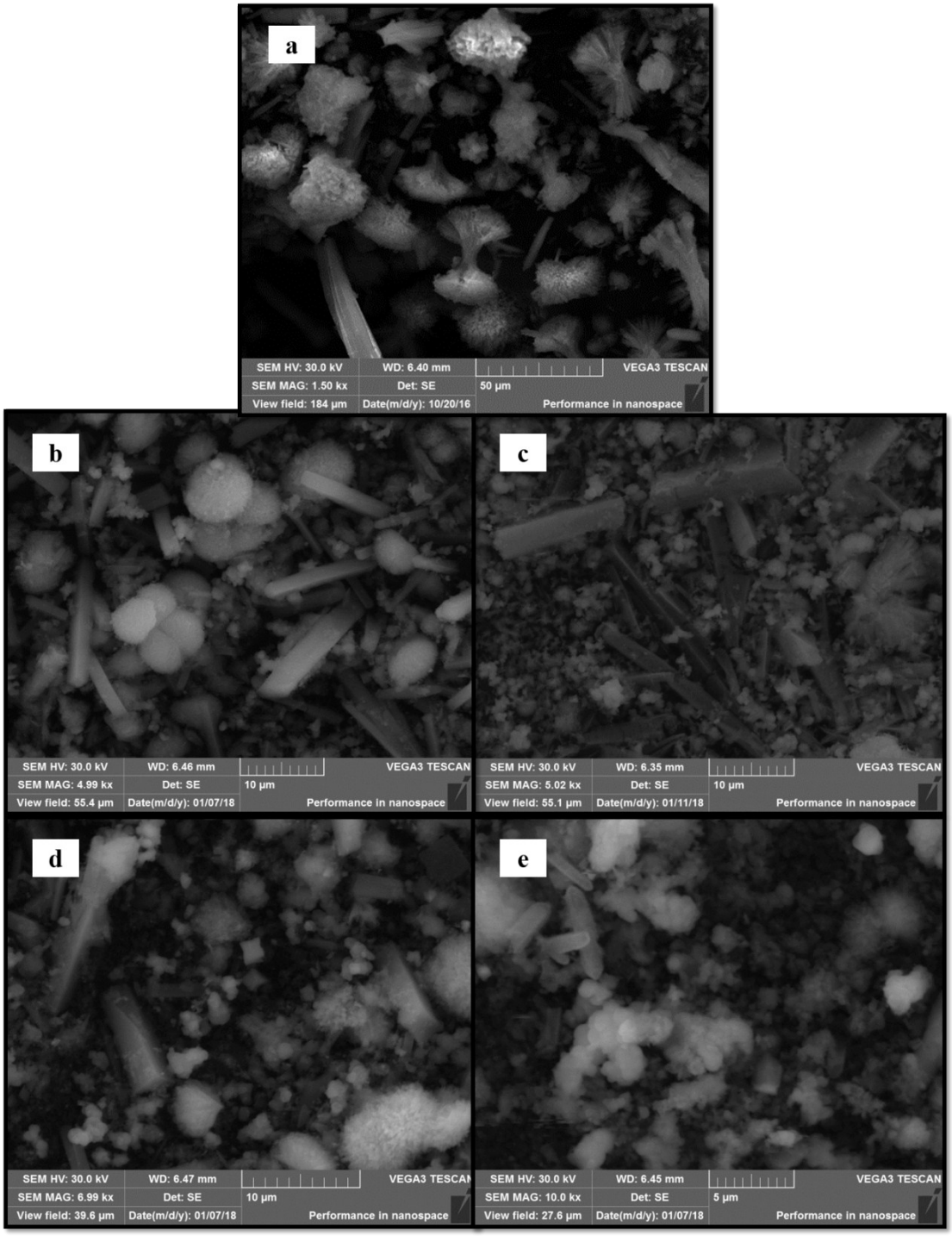

Fig. S4 SEM images of CeBTC (a), CeCuBTC-2 (b), CeCuBTC-5 (c), CeCuBTC-10 (d) and CeCuBTC-20 (e).

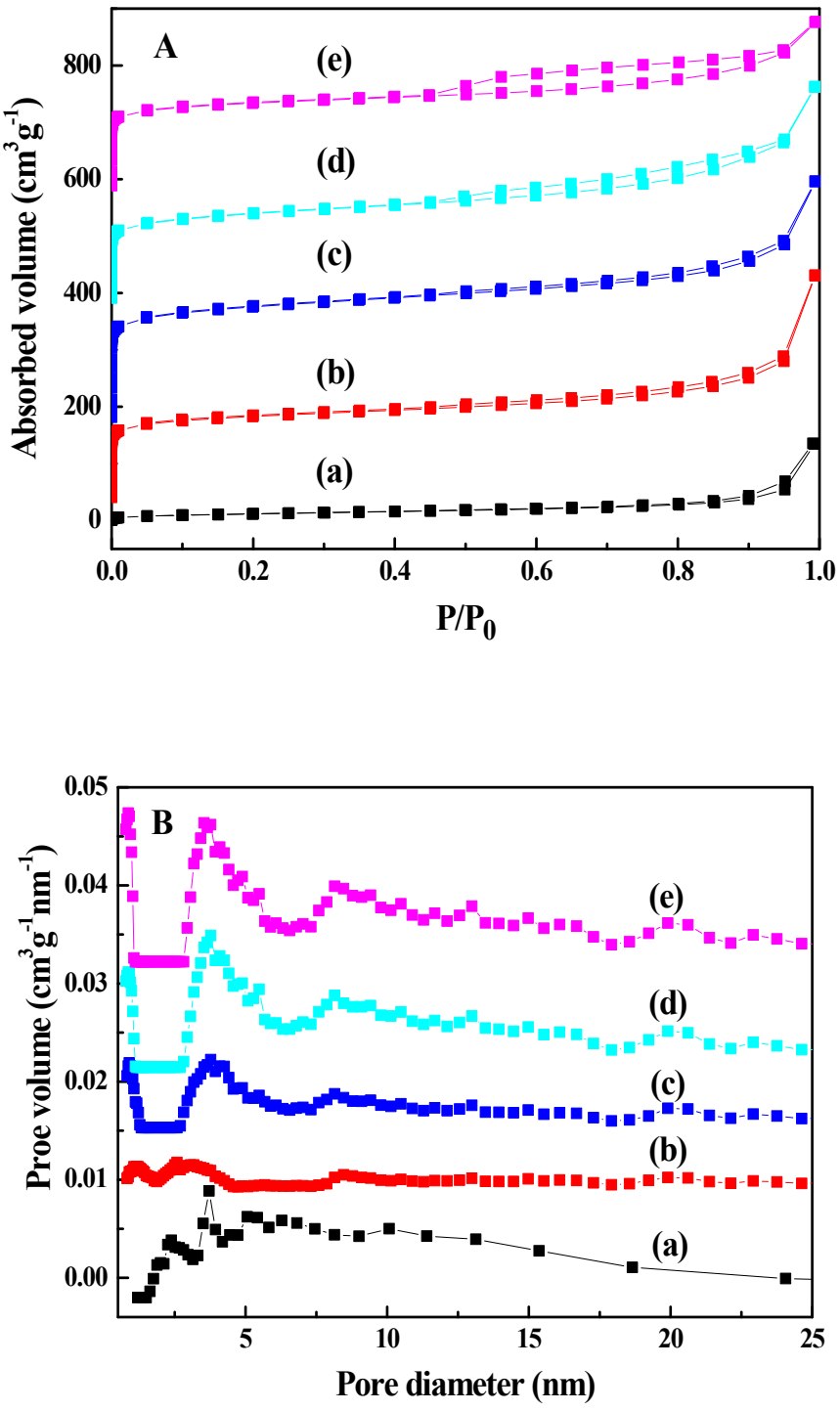

Fig. S5 N_2 adsorption-desorption isotherms (A) and corresponding pore size distributions (B) of CeO_2 (a), CuCeO-2 (b), CuCeO-5 (c), CuCeO-10 (d) and CuCeO-20 (e).

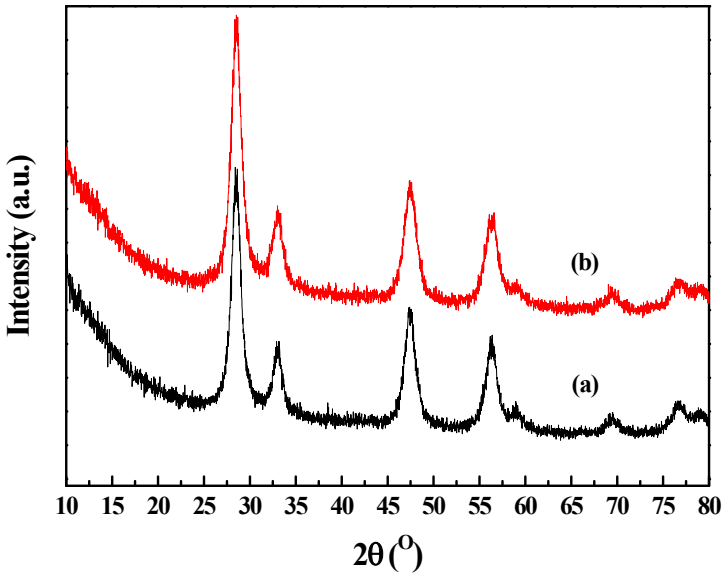

Fig. S6 XRD results of CuCeO-5 before (a) and after (b) CO oxidation reaction

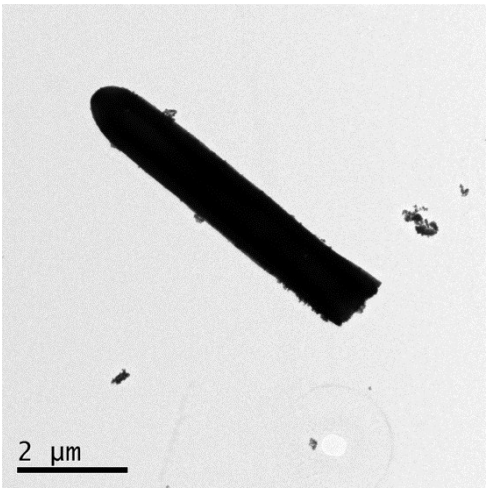

Fig. S7 TEM result of CuCeO-5 after CO oxidation reaction

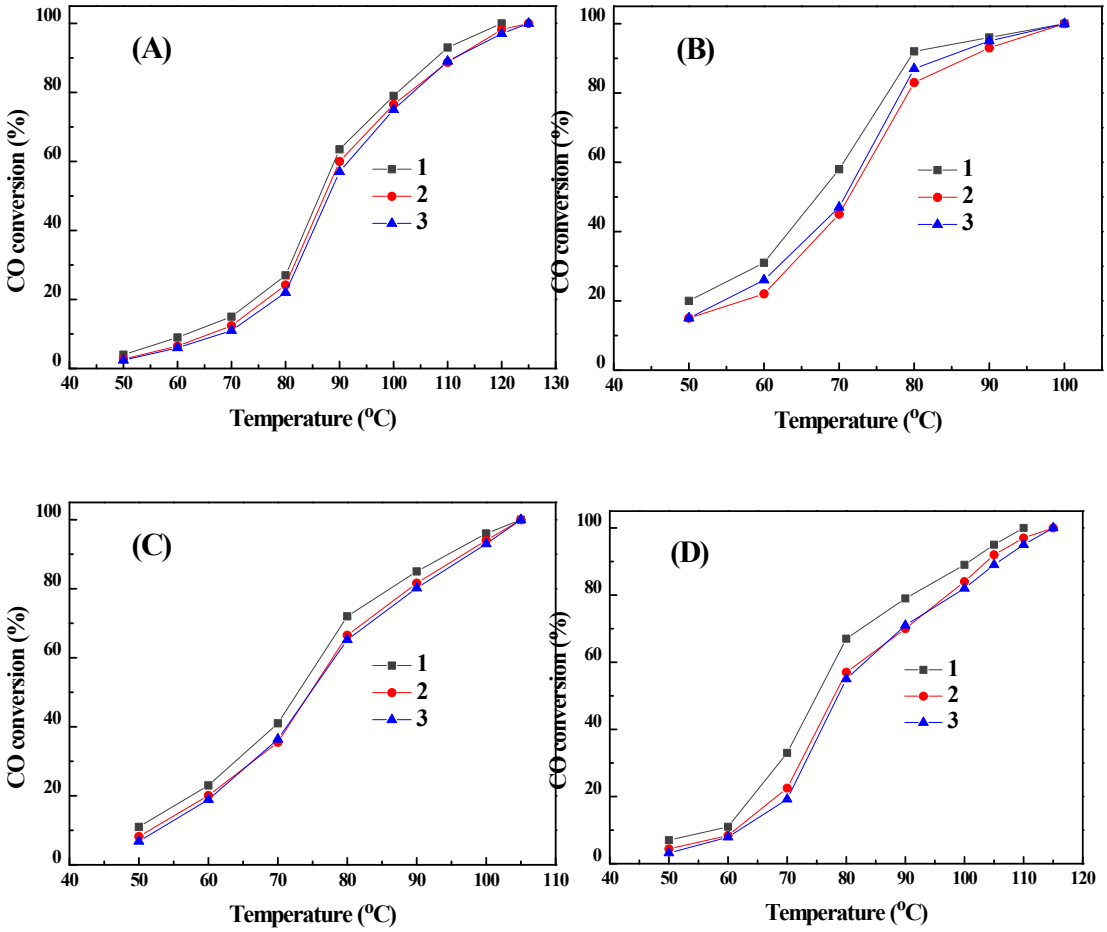

Fig. S8 Catalytic activities for CO oxidation of CuCeO-2 (A), CuCeO-5 (B), CuCeO-10 (C) and CuCeO-20 (D) reused for three times

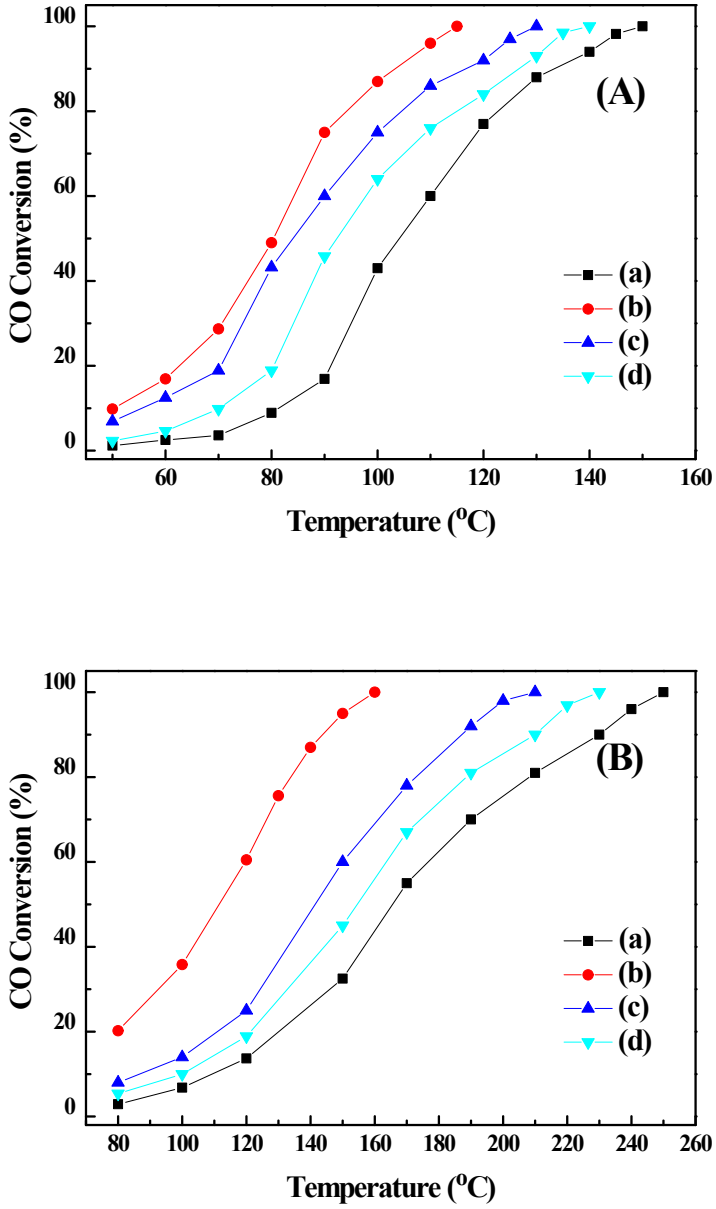

Fig. S9 catalytic activities for CO oxidation at different space velocities (30000 mL h^{-1} g^{-1} (A), 60000 mL h^{-1} g^{-1} (B)) of CuCeO-2 (a), CuCeO-5 (b), CuCeO-10 (c) and CuCeO-20 (d).